International Journal of Current Science Research and Review
ISSN: 2581-8341
Volume 09 Issue 07 July 2026
DOI: 10.47191/ijcsrr/V9-i7-27, Impact Factor: 8.048
IJCSRR @ 2026
www.ijcsrr.org

Linking Empirical Nickel Laterite Leaching Responses to Preliminary Economic Performance: Trade-Offs among Ni-Co Extraction, Acid Dosage, Fe Dissolution, and Residence Time

Antonio Clareti Pereira, PhD
PhD in Chemical Engineering
University of São Paulo (USP)
Belo Horizonte, Minas Gerais, Brazil
ORCID: https://orcid.org/0000-0001-8115-4279

ABSTRACT: This revised manuscript develops a transparent metallurgical-economic screening framework for atmospheric sulfuric acid leaching of a ferruginous nickel laterite ore. The objective is not to prove a universal kinetic mechanism or a final project-level feasibility estimate, but to evaluate how experimentally observed extraction responses translate into preliminary economic ranking under clearly stated assumptions. Duplicate leaching tests were performed at 95-100 °C using sulfuric acid dosages of 700-1000 kg H_2SO_4/t ore and residence times of 30-420 min. The tables report average values used for mass-balance and screening calculations; individual duplicate results are not shown in the main text, and formal significance claims are therefore avoided. Nickel and iron responses were modeled empirically as functions of acid dosage and residence time, while cobalt was included as a revenue component in selected base-case scenarios. The results show that the highest observed Ni extraction, 74.1% at 360 min and 1000 kg H_2SO_4/t ore, also produced the highest Fe dissolution, 65.8%, and a low Ni/Fe selectivity indicator. Under the base-case economic assumptions, the most attractive evaluated scenario was 420 min and 700 kg H_2SO_4/t ore, because the lower acid-addition cost and Fe penalty offset the lower Ni and Co extraction. Sensitivity analysis confirmed that this ranking is assumption-dependent and should be interpreted as a feasibility-screening result rather than a global economic optimum. Non-monotonic extraction behavior between 360 and 420 min is discussed cautiously as a possible combination of experimental dispersion, sampling effects, and secondary Ni retention associated with Fe(III) hydrolysis and sulfate-bearing phases. The revised framework provides a practical route for converting duplicated laboratory leaching tests into auditable, assumption-sensitive screening inputs for early-stage nickel laterite project evaluation.

KEYWORDS: nickel laterite; atmospheric sulfuric acid leaching; empirical modeling; acid dosage; iron dissolution; economic screening; Ni/Fe selectivity; feasibility studies.

HIGHLIGHTS

- Duplicate leaching tests were used to support exploratory metallurgical-economic screening.
- The study ranks leaching scenarios rather than claiming mechanistic kinetic proof.
- Higher Ni extraction increased Fe dissolution, acid-addition cost, and capital intensity.
- The best base-case scenario was not the condition of maximum observed Ni extraction.
- Secondary Ni retention is discussed as plausible but not directly proven.

International Journal of Current Science Research and Review
ISSN: 2581-8341
Volume 09 Issue 07 July 2026
DOI: 10.47191/ijcsrr/V9-i7-27, Impact Factor: 8.048
IJCSRR @ 2026
www.ijcsrr.org

Graphical abstract

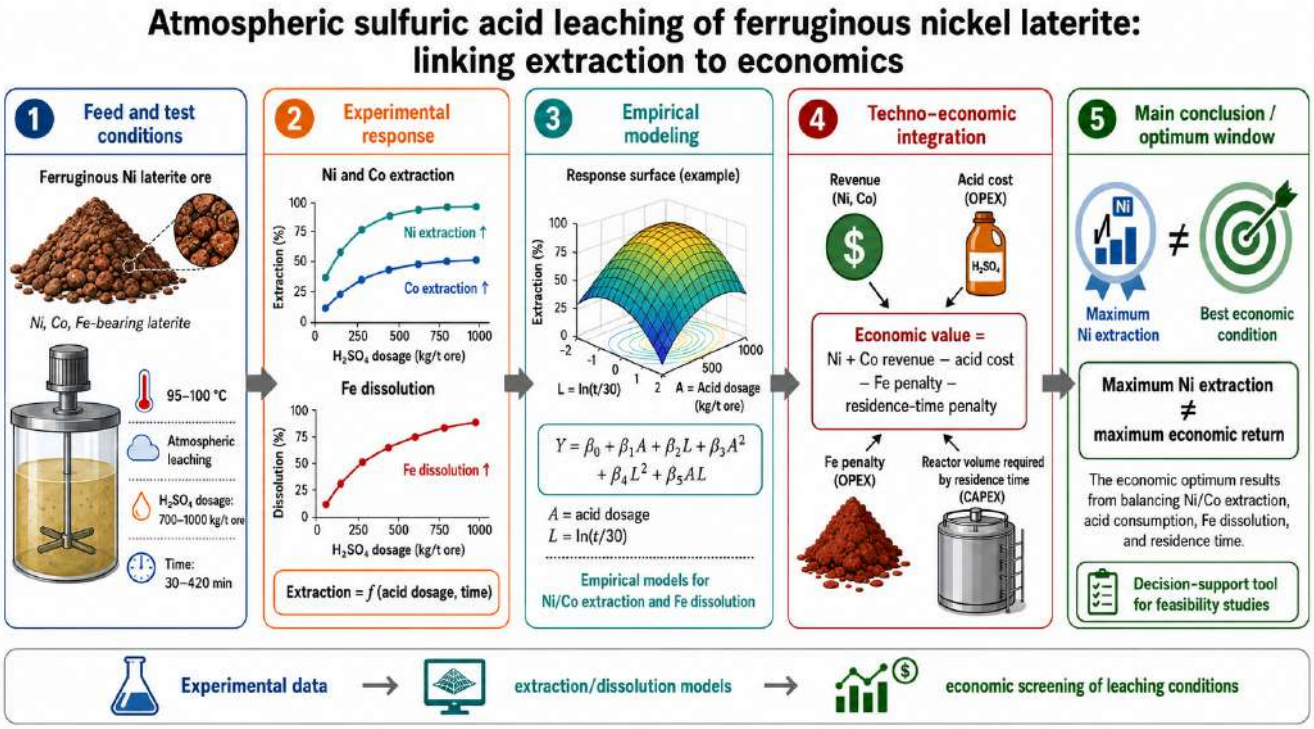

1. INTRODUCTION

Nickel is a strategic metal for stainless steels, superalloys, and battery supply chains, and the expansion of low-carbon technologies has intensified the need for secure and sustainable nickel resources (Basuhi et al., 2024; Foss & Koelsch, 2022; Msumange et al., 2026). Lateritic nickel ores represent a major resource base, but their processing remains challenging because Ni and Co are commonly distributed among iron oxyhydroxides, clay minerals, serpentine, poorly crystalline Fe-Si phases, and manganese oxides (Acquah et al., 2025, 2026; Bonfu et al., 2026; Caetano et al., 2025).

Hydrometallurgical options for laterites include pressure acid leaching, atmospheric acid leaching, heap leaching, bioleaching, chloride leaching, sulfation roasting followed by water leaching, and combined beneficiation-leaching strategies. These routes involve different trade-offs among Ni-Co extraction, reagent addition, selectivity, residue generation, scale-up risk, OPEX, and CAPEX (Agatzini-Leonardou et al., 2021; Chi et al., 2026; Duman & Can, 2022; Stankovic et al., 2022; Suleimen et al., 2026). Pressure acid leaching can produce high extraction from limonitic ores, but it requires autoclaves, stringent materials of construction, and complex scale-up control (Connelly, 2025; Duman & Can, 2022). Atmospheric sulfuric acid leaching is simpler but often requires high acid dosage and long residence time, especially for ferruginous and mineralogically heterogeneous ores (Jeong et al., 2025; Kang et al., 2026; Lasut et al., 2023; Ribeiro et al., 2025; Santos et al., 2021).

For ferruginous laterites, the main process challenge is not only Ni extraction but also the simultaneous dissolution of Fe. Iron dissolution increases acid demand, neutralization load, impurity-removal burden, residue generation, and the risk of Ni and Co losses during purification. This selectivity challenge has been emphasized in recent work on Fe-rich leach liquors and laterite processing residues (Boafo et al., 2026; Lei et al., 2020; Prameswara et al., 2025; Wang et al., 2025; Wen et al., 2025). Therefore, the most attractive leaching condition cannot be selected from Ni extraction alone; it must consider the marginal value of additional Ni and Co against marginal acid addition, Fe dissolution, and residence-time-related reactor volume.

A second issue is the interpretation of non-monotonic extraction behavior in Fe-rich sulfate systems. Apparent decreases in dissolved Ni after longer reaction times may arise from experimental dispersion, sequential sampling, mass-balance uncertainty, or secondary retention mechanisms. Fe(III) hydrolysis and precipitation can promote adsorption, occlusion, or co-precipitation of Ni in Fe-rich or sulfate-bearing secondary phases (Pereira, 2026a). A $BaCl_2$ diagnostic study showed that a limited but measurable fraction of residual Ni in atmospheric sulfuric leaching residues could be remobilized under sulfate-scavenging

International Journal of Current Science Research and Review
ISSN: 2581-8341
Volume 09 Issue 07 July 2026
DOI: 10.47191/ijcsrr/V9-i7-27, Impact Factor: 8.048
IJCSRR @ 2026
www.ijcsrr.org

conditions, supporting the plausibility of sulfate-related Ni retention, though it did not provide direct mineralogical evidence (Pereira, 2026b).

This study addresses the gap between laboratory leaching tests and early-stage project screening. The framework is consistent with the principles of circular and sustainable hydrometallurgy, which emphasize reagent efficiency, impurity control, residue minimization, and integration of metallurgical responses into economic decision-making (Binnemans & Jones, 2023; Botelho Junior et al., 2023; Kalupahana et al., 2025; O'Sullivan & Williams, 2024). The specific objectives are to: (i) quantify the effects of sulfuric acid dosage and residence time on Ni extraction and Fe dissolution; (ii) fit empirical interpolation equations for screening; (iii) include selected Co values in base-case revenue calculations; (iv) compare metallurgical and economic rankings; and (v) define a cautious decision-support workflow that recognizes statistical and economic uncertainty.

2. MATERIALS AND METHODS

2.1. Ore sample and experimental basis

The experimental study was performed using a ferruginous nickel laterite ore fraction retained on a 100-mesh sieve. Each leaching test used 600 g of ore. Atmospheric sulfuric acid leaching was conducted at approximately 95-100 °C under mechanical agitation for residence times up to 420 min. The experimental matrix was designed to test four sulfuric acid concentrations while maintaining the same initial ore and slurry masses.

Table 1 presents the acid-dosage matrix. The H_2SO_4 mass ranged from 420 to 600 g, corresponding to 700-1000 kg H_2SO_4/t ore. Water addition was adjusted to maintain a constant initial slurry mass of 3000 g.

Table 1. Sulfuric acid dosage matrix used in the leaching tests.

Test	Ore mass (g)	H_2SO_4 mass (g)	Water mass (g)	H_2SO_4 dosage (kg/t ore)
1	600	420	1980	700
2	600	480	1920	800
3	600	540	1860	900
4	600	600	1800	1000

Source: Authors' own elaboration based on the experimental leaching test design.

This matrix enabled the evaluation of the effect of acid dosage while keeping the ore mass and the total initial slurry mass constant. Differences in Ni extraction and Fe dissolution can therefore be interpreted primarily in terms of acid dosage, residence time, and ore response under the defined experimental conditions.

2.2. Chemical composition of the ore

Table 2 presents the head composition used for mass-balance and extraction calculations. The ore is Fe-rich and contains relatively low Ni and Co grades, consistent with a ferruginous lateritic nickel ore.

Table 2. Head composition used in the extraction calculations.

Element	Content (wt.%)
Al	1.9402
Ca	0.0966
Co	0.0667
Cr	1.9653
Cu	0.0100
Fe	34.4925
Mg	3.8229
Mn	0.6455
Ni	0.8975
Si	11.7176
Zn	0.0300

Source: Authors' own elaboration based on the chemical characterization of the ore sample.

International Journal of Current Science Research and Review
ISSN: 2581-8341
Volume 09 Issue 07 July 2026
DOI: 10.47191/ijcsrr/V9-i7-27, Impact Factor: 8.048
IJCSRR @ 2026
www.ijcsrr.org

For one tonne of ore, these grades correspond to approximately 8.975 kg Ni/t, 0.667 kg Co/t, and 344.925 kg Fe/t. These values were used to convert extraction percentages into metal masses and dissolved impurity loads.

2.3. Leaching data treatment and mass-balance basis

For each sampling point, the leach liquor, wash water, and residue were analyzed. Extraction was calculated as the combined contribution of the pregnant leach solution and wash liquor to avoid underestimating the dissolved metal retained in the wet residue before washing. The acid dosage and logarithmic residence-time variables are defined as follows (Eq. 1):

$$A = (D - 700) / 100 \quad (1)$$

$$L = \ln(t / 30) \quad (2)$$

where D is sulfuric acid dosage in kg H_2SO_4/t ore, t is residence time in min, A is the coded acid-dosage variable, and L is the logarithmic time variable.

$$V_L = m_L / (\rho_L \times 1000) \quad (3)$$

$$V_W = m_W / (\rho_W \times 1000) \quad (4)$$

$$m_{i,diss} = C_{i,L} V_L + C_{i,W} V_W \quad (5)$$

$$m_{ore,dry} = m_{pulp} S (1 - M) \quad (6)$$

$$m_{i,0} = m_{ore,dry} (G_i / 100) \quad (7)$$

$$X_i = (m_{i,diss} / m_{i,0}) \times 100 \quad (8)$$

In Eqs. (3)-(8), V_L and V_W are the liquor and wash-water volumes, ρ_L and ρ_W are the corresponding liquid densities, $C_{i,L}$ and $C_{i,W}$ are element concentrations, $m_{i,diss}$ is the dissolved mass of element i, $m_{i,0}$ is the initial mass of element i in the represented dry ore, and X_i is the calculated extraction or dissolution percentage. For Ni and Co, X_i is interpreted as extraction into solution. For Fe, X_i is interpreted as the dissolution of impurities.

2.4. Statistical treatment and scope of inference

The experimental work was performed in duplicate. The values reported in the main tables are the averages used for the mass-balance calculations and the economic screening exercise. The individual duplicate results are not shown in the main text; therefore, the manuscript does not claim statistical significance for differences among individual leaching conditions. The duplicate tests were used to support confirmation of process trends and internal consistency checks, whereas the central objective of the article is to compare the relationship between metallurgical response and economic index under transparent assumptions.

This distinction matters. The manuscript's purpose isn't to establish a definitive acid consumption value, a universal kinetic law, or a mechanistic Ni extraction model. Instead, it shows how duplicated laboratory leaching responses can serve as preliminary feasibility indicators. Terms like "significant increase" are avoided unless supported by numerical contrasts, and R^2 values are only seen as measures of interpolation fit within the tested domain. Fixed-time and fixed-dosage regressions are used as visual aids, not as independent predictive models.

2.5. Experimental extraction matrix

The extraction data used for the empirical modeling are summarized in Tables 3 and 4. The values correspond to the combined recovery of leach liquor and wash water. Ni and Fe are reported in full because Ni is the main revenue-generating metal and Fe is the main impurity penalty. Co was included in the selected economic scenarios as an additional revenue-generating metal; selected Co values are shown in Table 5.

Table 3. Nickel extraction as a function of time and acid dosage (%).

Time (min)	700 kg/t	800 kg/t	900 kg/t	1000 kg/t
30	38.9	42.1	50.0	52.1
60	45.2	57.8	52.8	52.6
120	54.4	57.4	60.9	67.3
240	58.2	63.2	69.3	64.3
300	58.4	58.9	61.0	70.3
360	58.9	65.5	70.0	74.1
420	66.2	71.1	61.3	72.9

Source: Authors' own elaboration based on the experimental leaching data.

International Journal of Current Science Research and Review
ISSN: 2581-8341
Volume 09 Issue 07 July 2026
DOI: 10.47191/ijcsrr/V9-i7-27, Impact Factor: 8.048
IJCSRR @ 2026
www.ijcsrr.org

Table 4. Iron dissolution as a function of time and acid dosage (%).

Time (min)	700 kg/t	800 kg/t	900 kg/t	1000 kg/t
30	21.2	24.4	30.5	34.6
60	25.6	36.8	35.1	37.4
120	32.7	38.9	42.3	52.3
240	36.3	45.9	52.6	54.8
300	37.7	43.0	45.1	61.1
360	37.6	48.0	55.4	65.8
420	42.9	52.3	47.4	63.1

Source: Authors' own elaboration based on the experimental leaching data.

Table 5. Selected co-extraction values used in the base-case economic simulation.

Condition	Ni (%)	Co (%)	Fe (%)
420 min / 700 kg/t	66.2	41.4	42.9
420 min / 800 kg/t	71.1	44.8	52.3
360 min / 800 kg/t	65.5	40.9	48.0
240 min / 700 kg/t	58.2	31.0	36.3
240 min / 900 kg/t	69.3	39.3	52.6
360 min / 1000 kg/t	74.1	47.1	65.8

Source: Authors' own elaboration based on selected metallurgical results used for the scenario calculation.

The extraction matrix shows that Ni extraction generally increased with residence time and acid dosage. However, the response was not strictly monotonic. For example, the 900 kg/t condition decreased from 70.0% Ni at 360 min to 61.3% at 420 min. Such behavior is treated cautiously and may reflect a combination of experimental dispersion, sampling effects, mass-balance uncertainty, and secondary Ni retention associated with Fe-rich or sulfate-bearing phases.

2.6. Empirical response modeling

The experimental responses were modeled using empirical interpolation equations. These equations are not mechanistic kinetic laws and should not be used outside the experimental domain. The general response model is:

$$X_M = \beta_0 + \beta_1 A + \beta_2 L + \beta_3 A^2 + \beta_4 L^2 + \beta_5 A L \quad (9)$$

Where X_M is the response for element M. The logarithmic-time term represents rapid initial dissolution, followed by slower marginal extraction at longer residence times.

$$X_{Ni} = 39.75 + 4.63A + 11.11L - 0.268A^2 - 0.970L^2 - 0.333AL \quad (10)$$

$$X_{Co} = 14.40 + 2.70A + 6.54L + 0.175A^2 + 0.961L^2 - 0.130AL \quad (11)$$

$$X_{Fe} = 21.86 + 3.31A + 8.14L + 0.193A^2 - 0.376L^2 + 1.312AL \quad (12)$$

Table 6. Summary of empirical response equations and scope of use.

Element	Equation	R^2	Interpretation and limitation
Ni	Eq. (10)	0.86	Primary metallurgical response: screening interpolation only.
Co	Eq. (11)	0.94	Auxiliary revenue response: selected Co values are shown for audited scenarios.
Fe	Eq. (12)	0.93	The impurity dissolution response is treated as both OPEX and a selectivity penalty.

Source: Authors' own elaboration based on empirical response models derived from duplicate-average leaching data.

The R^2 values indicate that the equations reproduce the main trends within the studied domain, but they should be interpreted with caution. Because the article focuses on feasibility screening rather than kinetic mechanism validation, the models

International Journal of Current Science Research and Review
ISSN: 2581-8341
Volume 09 Issue 07 July 2026
DOI: 10.47191/ijcsrr/V9-i7-27, Impact Factor: 8.048
IJCSRR @ 2026
www.ijcsrr.org

are used to compare relative responses and to perform economic ranking, not to establish reaction orders, activation energies, or mineral-specific rate constants.

2.7. Fixed-dosage and fixed-time functions

For interpretive purposes, fixed-dose-time functions and fixed-time acid-dose functions were also fitted. They were retained as descriptive summaries of the marginal effects of residence time and acid dosage. Because some of these regressions use a small number of points, high R^2 values should not be interpreted as independent validation.

$X_M = a + bL + cL^2$ (13)

Table 7. Numbered fixed-dosage time functions for nickel extraction.

Dosage	Function	Eq.	R^2
700 kg/t	$X_{Ni} = 38.94 + 10.38L - 0.501L^2$	(14)	0.95
800 kg/t	$X_{Ni} = 44.62 + 12.33L - 1.555L^2$	(15)	0.81
900 kg/t	$X_{Ni} = 48.45 + 12.21L - 2.201L^2$	(16)	0.73
1000 kg/t	$X_{Ni} = 51.02 + 7.51L + 0.377L^2$	(17)	0.87

Source: Authors' own elaboration based on duplicate-average Ni extraction data.

Table 8. Numbered fixed-dosage time functions for iron dissolution.

Dosage	Function	Eq.	R^2
700 kg/t	$X_{Fe} = 21.15 + 7.25L + 0.077L^2$	(18)	0.97
800 kg/t	$X_{Fe} = 25.95 + 11.51L - 1.021L^2$	(19)	0.92
900 kg/t	$X_{Fe} = 29.47 + 11.69L - 1.325L^2$	(20)	0.83
1000 kg/t	$X_{Fe} = 33.47 + 9.98L + 0.764L^2$	(21)	0.95

Source: Authors' own elaboration based on duplicate-average Fe dissolution data.

$X_M = a + bA + cA^2$ (22)

Table 9. Numbered fixed-time acid-dosage functions for nickel extraction.

Time	Function	Eq.	R^2
30 min	$X_{Ni} = 38.38 + 5.58A - 0.275A^2$	(23)	0.95
60 min	$X_{Ni} = 46.32 + 11.32A - 3.20A^2$	(24)	0.69
120 min	$X_{Ni} = 54.52 + 1.67A + 0.850A^2$	(25)	1.00
240 min	$X_{Ni} = 57.59 + 9.94A - 2.50A^2$	(26)	0.88
300 min	$X_{Ni} = 58.68 - 2.82A + 2.20A^2$	(27)	0.98
360 min	$X_{Ni} = 58.99 + 6.89A - 0.625A^2$	(28)	1.00
420 min	$X_{Ni} = 68.01 - 4.00A + 1.68A^2$	(29)	0.20

Source: Authors' own elaboration based on the experimental Ni extraction data and fixed-time polynomial regression.

Table 10. Numbered fixed-time acid-dosage functions for iron dissolution.

Time	Function	Eq.	R^2
30 min	$X_{Fe} = 20.94 + 4.00A + 0.217A^2$	(30)	0.99
60 min	$X_{Fe} = 26.49 + 10.00A - 2.210A^2$	(31)	0.84
120 min	$X_{Fe} = 33.14 + 3.42A + 0.932A^2$	(32)	0.98
240 min	$X_{Fe} = 36.22 + 11.74A - 1.839A^2$	(33)	1.00
300 min	$X_{Fe} = 38.52 - 0.81A + 2.684A^2$	(34)	0.95
360 min	$X_{Fe} = 37.86 + 9.27A - 0.024A^2$	(35)	1.00
420 min	$X_{Fe} = 44.69 + 0.80A + 1.581A^2$	(36)	0.73

Source: Authors' own elaboration based on the experimental Fe dissolution data and fixed-time polynomial regression.

International Journal of Current Science Research and Review
ISSN: 2581-8341
Volume 09 Issue 07 July 2026
DOI: 10.47191/ijcsrr/V9-i7-27, Impact Factor: 8.048
IJCSRR @ 2026
www.ijcsrr.org

The 420 min Ni function has a very low R^2 and is therefore interpreted only as a descriptive curve. The Fe functions show a generally stronger and more consistent response to acid dosage, reinforcing that additional acid may increase impurity dissolution as well as Ni extraction.

2.8. Economic screening model

The empirical and experimental responses were converted into a simplified economic screening index. The model is comparative and should not be interpreted as a final feasibility estimate. It uses acid-addition cost rather than measured acid consumption because residual free acid and recoverable acid were not measured in this dataset.

$$R_{Ni+Co} = m_{Ni,0} (X_{Ni}/100) P_{Ni} + mC_{o,0} (X_{Co}/100) P_{Co} \quad (37)$$

$$C_{acid,add} = D P_{acid} f_{acid} \quad (38)$$

$$C_{Fe} = m_{Fe,0} (X_{Fe}/100) C_{Fe,treat} \quad (39)$$

$$C_{time} = C_h (t/60) \quad (40)$$

$$I_{econ} = R_{Ni+Co} - C_{acid,add} - C_{Fe} - C_{time} \quad (41)$$

In Eq. (38), f_{acid} is the fraction of added acid charged to the economic scenario. The base case uses $f_{acid} = 1.00$, while sensitivity cases use lower values to represent potential residual acidity, acid recycle, or partial acid recovery. The time term is an empirical residence-time penalty and not an annualized CAPEX estimate.

Table 11. Relative reactor volume and CAPEX factor using 120 min as reference.

Time (min)	Relative volume	Relative CAPEX factor
30	0.25	0.44
60	0.50	0.66
120	1.00	1.00
240	2.00	1.52
300	2.50	1.73
360	3.00	1.93
420	3.50	2.12

Source: Authors' own elaboration based on residence-time scaling and the six-tenths rule used as a conceptual indicator.

Table 12. Economic assumptions used in the base-case simulation.

Parameter	Value
Ni price	US$ 16/kg Ni
Co price	US$ 30/kg Co
H_2SO_4 addition cost	US$ 0.08/kg H_2SO_4
Fe treatment penalty	US$ 0.03/kg Fe dissolved
Empirical residence-time penalty	US$ 1.50/h/t ore

Source: Authors' own assumptions used only for comparative economic screening.

3. RESULTS AND DISCUSSION

3.1. Nickel extraction response

Figure 1 shows the average Ni extraction values as a function of residence time for the four sulfuric acid dosages. Ni extraction increased from 38.9-52.1% at 30 min to higher values at longer residence times, reaching the maximum observed value of 74.1% at 360 min and 1000 kg H_2SO_4/t ore. The data also show non-monotonic behavior at selected conditions, especially between 360 and 420 min.

International Journal of Current Science Research and Review
ISSN: 2581-8341
Volume 09 Issue 07 July 2026
DOI: 10.47191/ijcsrr/V9-i7-27, Impact Factor: 8.048
IJCSRR @ 2026
www.ijcsrr.org

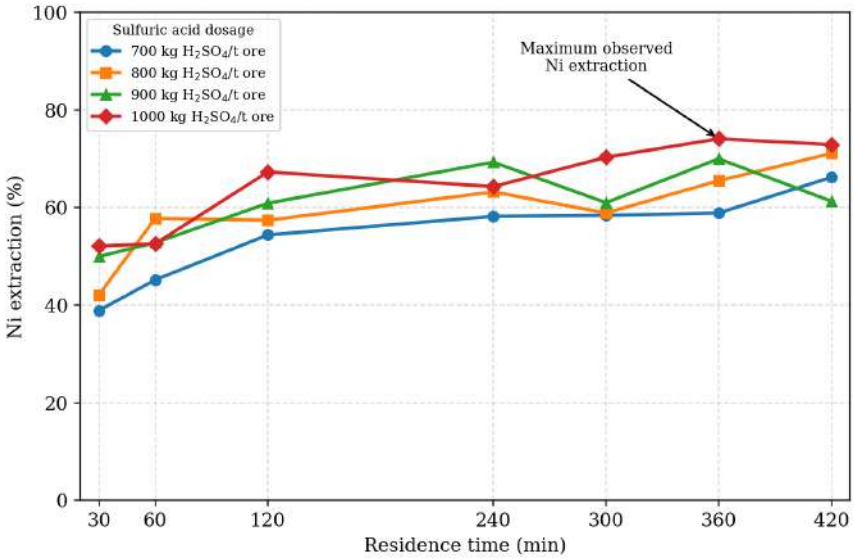

Figure 1. Nickel extraction as a function of residence time at fixed sulfuric acid dosages. Source: Prepared by the authors from duplicate-averaged experimental results obtained in this study.

The apparent decrease in Ni between 360 and 420 min is not a simple reversal of dissolution. In Fe-rich sulfate systems, increased dissolved Fe can cause Fe(III) hydrolysis and secondary precipitation, which may trap Ni through adsorption, occlusion, co-precipitation, or sulfate retention. This is supported by co-precipitation principles and evidence of $BaCl_2$-remobilized Ni in similar residues (Pereira, 2026a, 2026b). However, without data on duplicate values, sulfate levels, or mineralogy, this explanation remains plausible rather than confirmed.

3.2. Iron dissolution and selectivity penalty

Figure 2 presents Fe dissolution under the same fixed acid dosages. Fe dissolution increased with both acid dosage and residence time, reaching 65.8% at 360 min and 1000 kg H_2SO_4/t ore. This condition also yielded the highest Ni extraction, illustrating the selectivity penalty associated with more aggressive leaching that dissolves the ferruginous matrix.

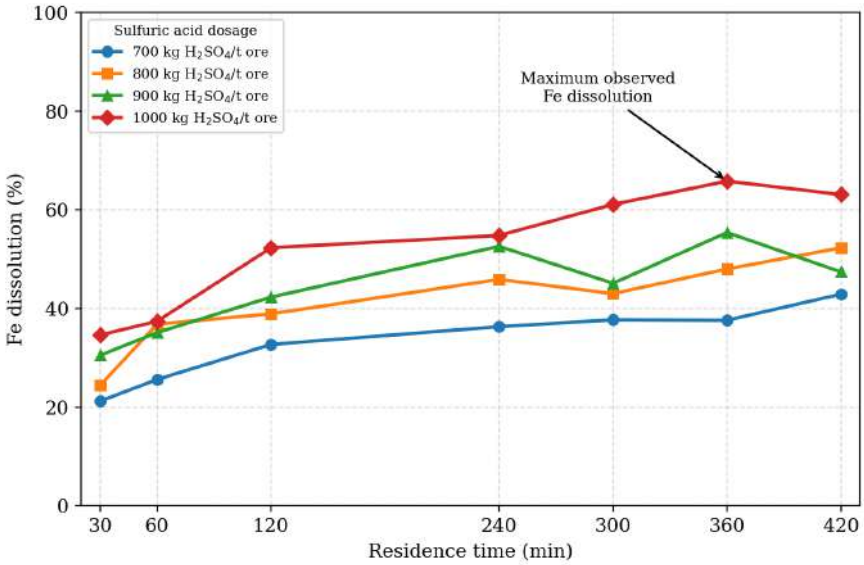

Figure 2. Iron dissolution as a function of residence time at fixed sulfuric acid dosages. Source: Prepared by the authors from duplicate-averaged experimental results obtained in this study.

International Journal of Current Science Research and Review
ISSN: 2581-8341
Volume 09 Issue 07 July 2026
DOI: 10.47191/ijcsrr/V9-i7-27, Impact Factor: 8.048
IJCSRR @ 2026
www.ijcsrr.org

A simple Ni/Fe selectivity indicator was calculated as $S_{Ni/Fe} = X_{Ni}/X_{Fe}$. Table 13 shows that the most selective condition among the selected examples was 420 min/700 kg/t, even though it did not yield the highest Ni extraction.

Table 13. Selected Ni/Fe selectivity indicators.

Condition	Ni extraction (%)	Fe dissolution (%)	$S_{Ni/Fe}$
420 min / 700 kg/t	66.2	42.9	1.54
420 min / 800 kg/t	71.1	52.3	1.36
240 min / 900 kg/t	69.3	52.6	1.32
360 min / 1000 kg/t	74.1	65.8	1.13

Source: Authors' own elaboration based on the Ni extraction and Fe dissolution matrices.

3.3. Empirical response surfaces

Figure 3 shows the empirical response surfaces for Ni extraction and Fe dissolution within the tested domain. The surfaces are interpolation tools and are not intended to represent mechanistic kinetics. The Ni surface indicates increasing extraction with acid dosage and residence time, whereas the Fe surface shows that impurity dissolution also intensifies under more aggressive conditions.

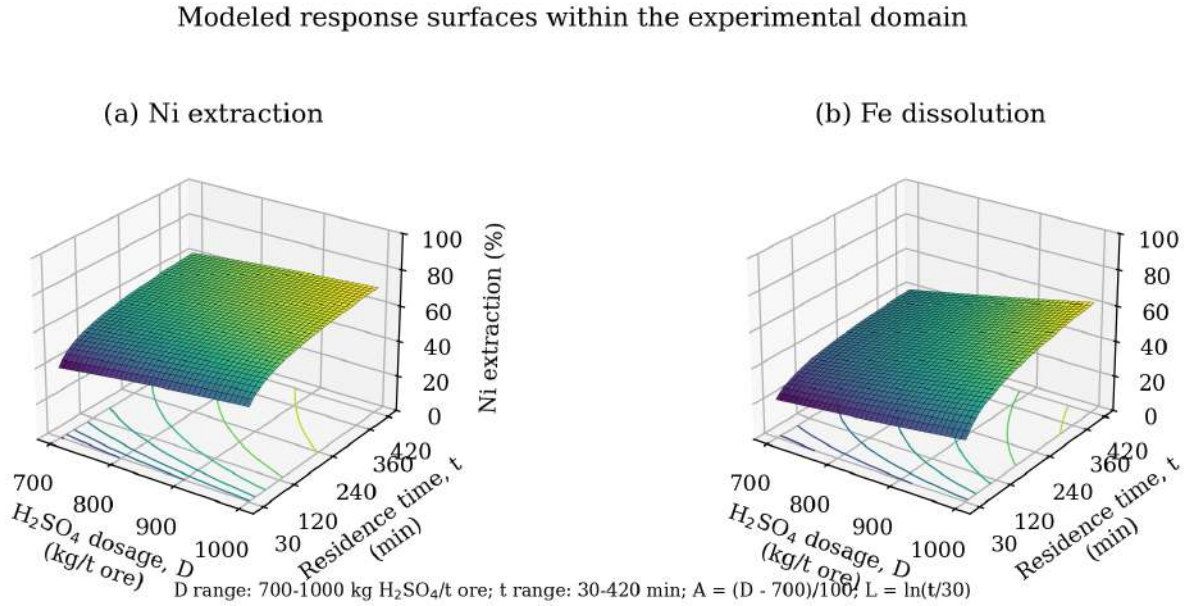

Figure 3. Modeled effects of sulfuric acid dosage and residence time on (a) Ni extraction and (b) Fe dissolution. The surfaces were generated within the experimental ranges of 700-1000 kg H_2SO_4/t ore and 30-420 min. Source: Authors' own elaboration based on the empirical response equations developed in this study.

Because these surfaces are based on empirical duplicate-average data rather than a mechanistic kinetic model, the results are most appropriate for screening, interpolation, and identifying trade-offs. They do not provide activation energies, rate constants, or mechanistic control regimes.

3.4. Fixed-time acid-dosage curves

Figure 4 presents the acid-dosage curves at fixed residence times. For Ni, additional acid generally increased extraction, but the marginal gain was not proportional at all residence times. For Fe, increasing acid dosage had a strong effect on dissolution, especially at longer residence times.

International Journal of Current Science Research and Review
ISSN: 2581-8341
Volume 09 Issue 07 July 2026
DOI: 10.47191/ijcsrr/V9-i7-27, Impact Factor: 8.048
IJCSRR @ 2026
www.ijcsrr.org

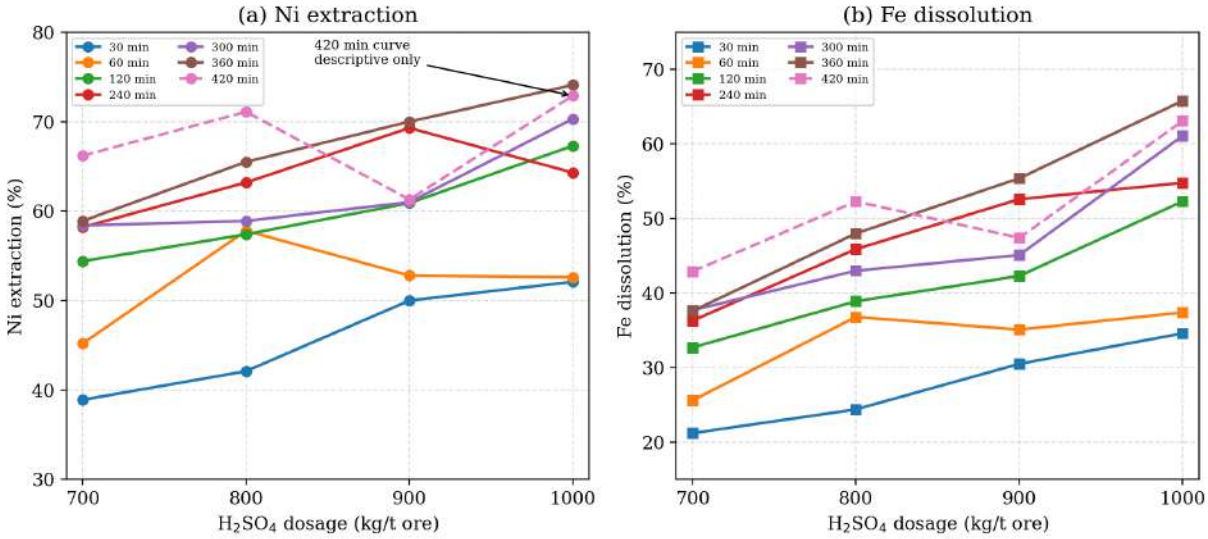

Figure 4. Acid-dosage curves for (a) Ni extraction and (b) Fe dissolution at fixed residence times. Lines are guides to the eye; the 420 min Ni curve is descriptive only. Source: Authors' own elaboration based on the experimental data and fixed-time acid-dosage functions.

These curves support the central trade-off of the study: higher acid dosage can improve Ni extraction but also increases Fe dissolution and acid-addition costs. Therefore, the operating condition should be selected by balancing extraction and penalties, not by maximizing Ni extraction alone.

3.5. Selected economic scenarios

Table 14 summarizes the metallurgical data used for the selected economic scenarios. Ni and Co contribute to revenue, whereas Fe dissolution contributes to treatment and selectivity penalties.

Table 14. Metallurgical results for selected economic scenarios.

Condition	Ni (%)	Co (%)	Fe (%)
420 min / 700 kg/t	66.2	41.4	42.9
420 min / 800 kg/t	71.1	44.8	52.3
360 min / 800 kg/t	65.5	40.9	48.0
240 min / 700 kg/t	58.2	31.0	36.3
240 min / 900 kg/t	69.3	39.3	52.6
360 min / 1000 kg/t	74.1	47.1	65.8

Source: Authors' own elaboration based on the selected experimental leaching scenarios.

Table 15. Economic indicators for selected scenarios (US$/t ore).

Condition	Revenue	Acid-addition cost	Fe penalty	Time penalty	Economic index
420 min / 700 kg/t	103.3	56.0	4.4	10.5	32.4
420 min / 800 kg/t	111.1	64.0	5.4	10.5	31.2
360 min / 800 kg/t	102.2	64.0	5.0	9.0	24.3
240 min / 700 kg/t	89.8	56.0	3.8	6.0	24.0
240 min / 900 kg/t	107.4	72.0	5.4	6.0	23.9
360 min / 1000 kg/t	115.8	80.0	6.8	9.0	20.0

Source: Authors' own elaboration based on selected metallurgical results and the economic-index formulation developed in this study.

International Journal of Current Science Research and Review
ISSN: 2581-8341
Volume 09 Issue 07 July 2026
DOI: 10.47191/ijcsrr/V9-i7-27, Impact Factor: 8.048
IJCSRR @ 2026
www.ijcsrr.org

Figure 5 shows the same economic index values for the selected base-case scenarios. The highest index was obtained at 420 min / 700 kg H_2SO_4/t ore. This condition did not produce the highest Ni extraction but provided the best balance among Ni and Co revenue, acid-addition cost, Fe dissolution, and residence-time penalty under the base-case assumptions.

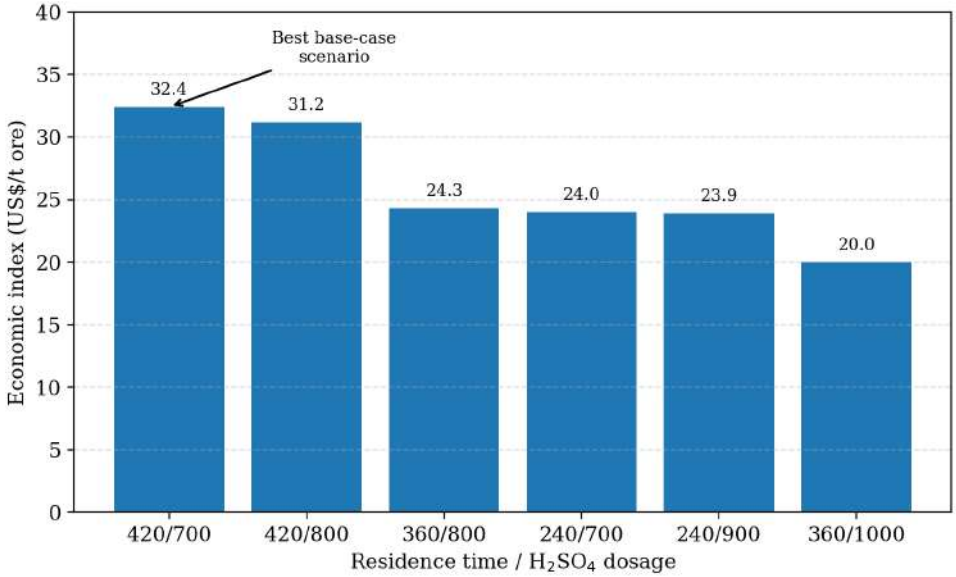

Figure 5. Economic index for selected leaching scenarios. Higher values indicate better base-case economic performance. Source: Authors' own elaboration based on Table 15.

3.6. Sensitivity to acid-cost allocation

Because acid dosage differs from measured acid consumption, a sensitivity analysis was performed using 100%, 75%, and 50% of the added acid charged to the economic index. This analysis addresses the possibility that part of the acid may remain as free acidity or become recyclable in a future flowsheet.

Table 16. Sensitivity of the economic index to the fraction of added acid charged to the scenario.

Condition	100% acid cost	75% acid cost	50% acid cost
420 min / 700 kg/t	32.4	46.4	60.4
420 min / 800 kg/t	31.2	47.2	63.2
360 min / 800 kg/t	24.3	40.2	56.2
240 min / 700 kg/t	24.0	38.0	52.0
240 min / 900 kg/t	23.9	42.0	60.0
360 min / 1000 kg/t	20.0	40.0	60.0

Source: Authors' own sensitivity calculation based on the same revenue, Fe penalty, and residence-time penalty shown in Table 15.

The sensitivity results show that the ranking is assumption-dependent. Under the base case, 420 min/700 kg/t is the best-selected scenario. If only 75% or 50% of acid addition is charged, 420 min / 800 kg/t becomes slightly more favorable. Therefore, the revised manuscript refers to the selected condition as the best base-case scenario among evaluated cases, not as a universal economic optimum.

3.7. Residence time, reactor volume, and capital intensity

Figure 6 shows the effect of residence time on relative reactor volume and a conceptual CAPEX factor. At fixed plant throughput, reactor volume is proportional to residence time. Increasing residence time from 120 to 420 min increases the relative

International Journal of Current Science Research and Review
ISSN: 2581-8341
Volume 09 Issue 07 July 2026
DOI: 10.47191/ijcsrr/V9-i7-27, Impact Factor: 8.048
IJCSRR @ 2026
www.ijcsrr.org

volume by a factor of 3.5. Using a six-tenths scaling indicator, the relative CAPEX factor becomes approximately 2.12. This is a conceptual reactor-volume scaling indicator, not a complete estimate of installed plant capital cost.

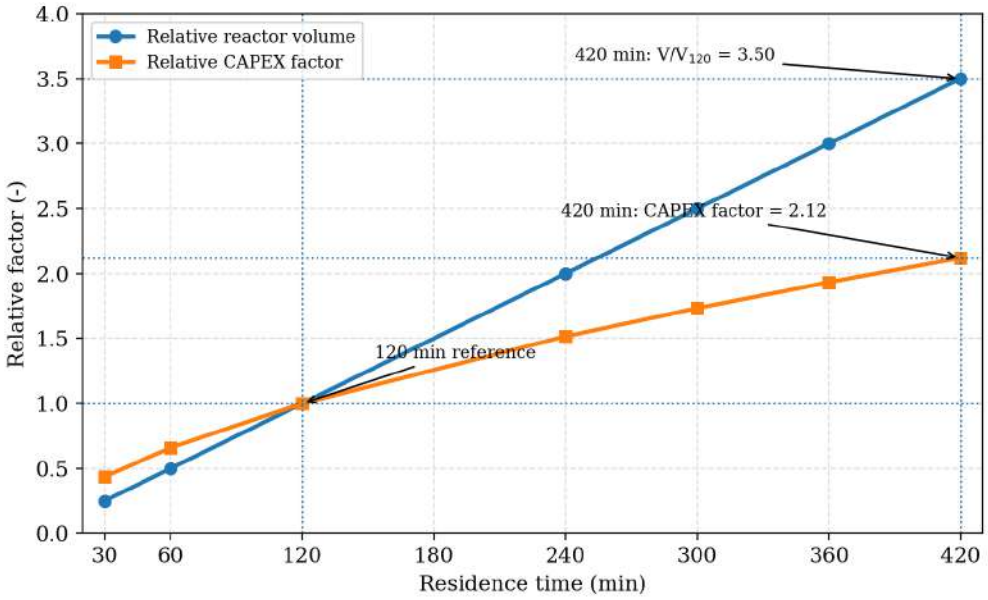

Figure 6. Relative reactor volume and CAPEX factor as a function of residence time. Source: Authors' own elaboration based on residence-time scaling and the six-tenths rule used as a conceptual indicator.

Table 17. Comparison between metallurgical and base-case economic optimum.

Criterion	Best condition	Ni (%)	Fe (%)	Economic meaning
Maximum Ni extraction	360 min / 1000 kg/t	74.1	65.8	Highest extraction, but high acid-addition cost and Fe penalty
Maximum base-case economic index	420 min / 700 kg/t	66.2	42.9	Lower extraction, but better cost/extraction balance

Source: Authors' own elaboration based on experimental leaching data and base-case economic index simulation.

The comparison confirms that maximum Ni extraction is not equivalent to maximum economic attractiveness. The most aggressive condition generated the highest revenue but also the highest acid cost and Fe penalty among the selected scenarios. The base-case economic ranking favored a less aggressive condition with better selectivity and lower operating penalties.

3.8. Decision-support workflow and limitations

Table 18 summarizes the revised decision-support workflow. The workflow is intended for preliminary feasibility screening and should be updated when full duplicate data, analytical uncertainty, free acid measurements, sulfate measurements, residue mineralogy, downstream recovery, payability, and plant-level CAPEX estimates become available.

Table 18. Decision-support workflow for transforming leaching tests into feasibility-screening inputs.

Step	Module	Purpose
1	Experimental leaching matrix	Vary the acid dosage and residence time; quantify the extraction of Ni, Co, Fe, and relevant impurities by mass balance.
2	Duplicate and uncertainty review	Report duplicate averages and, when available, individual values, standard deviations, analytical uncertainty, and mass-balance closure.
3	Empirical response models	Fit interpolation equations within the experimental domain and avoid extrapolation beyond tested conditions.

International Journal of Current Science Research and Review
ISSN: 2581-8341
Volume 09 Issue 07 July 2026
DOI: 10.47191/ijcsrr/V9-i7-27, Impact Factor: 8.048
IJCSRR @ 2026
www.ijcsrr.org

4	Revenue estimation	Convert Ni and Co extraction into recoverable metal masses, using downstream recovery and, when available, payability.
5	OPEX penalties	Convert acid addition to scenario cost, and Fe dissolution to treatment or neutralization penalty.
6	CAPEX linkage	Convert residence time into reactor volume and relative capital-intensity indicators.
7	Economic ranking	Rank conditions using an economic index or project-level metric. Distinguish selected-scenario best, observed best, and predicted optimum.
8	Sensitivity analysis	Test Ni price, Co price, acid cost, acid recovery, Fe penalty, downstream recovery, payability, and residence-time penalty.

Source: Authors' own elaboration based on the proposed metallurgical-economic screening framework.

The main limitations of this revised study are: (i) the main tables report duplicate-average values but not individual duplicate data; (ii) uncertainty bars are not shown; (iii) acid consumption was not measured directly, so acid-addition cost was used; (iv) the Co matrix is represented only by selected scenarios in the main text; (v) the time penalty is empirical rather than an annualized CAPEX calculation; and (vi) secondary Ni retention is a plausible mechanism but was not confirmed by complete post-leaching mineralogy for all residues. These limitations limit the strength of the conclusions but do not invalidate the central screening insight: the highest Ni extraction condition may not yield the most favorable economic outcome under realistic penalty assumptions.

4. CONCLUSIONS

- ✓ The revised manuscript presents the work as an exploratory metallurgical-economic screening study rather than a definitive kinetic or project-feasibility assessment.
- ✓ Ni extraction generally increased with acid dosage and residence time, but non-monotonic behavior occurred at selected conditions, especially between 360 and 420 min.
- ✓ The non-monotonic behavior is compatible with experimental dispersion, sampling effects, and possible secondary Ni retention in Fe-rich or sulfate-bearing phases; however, this mechanism is treated as plausible rather than proven.
- ✓ The highest observed Ni extraction was 74.1% at 360 min and 1000 kg H_2SO_4/t ore, but this condition also produced the highest Fe dissolution among the selected scenarios.
- ✓ Under the base-case assumptions, 420 min and 700 kg H_2SO_4/t ore were the best selected economic scenario, because lower acid-addition cost and Fe penalty outweighed the lower Ni and Co extraction.
- ✓ Sensitivity analysis showed that the economic ranking changes when the fraction of added acid charged to the scenario is reduced, demonstrating that the result is assumption-dependent.
- ✓ Future work should report individual duplicate results, mass-balance closures, standard deviations, free acidity, sulfate speciation, residue mineralogy, downstream recovery, payability, and annualized CAPEX.

DECLARATIONS

Funding: No external funding was received for this study.

Conflicts of interest: The author declares no conflicts of interest.

Data availability: The calculated tables are included in the manuscript. Individual duplicate datasets, raw analytical reports, and spreadsheet calculations should be provided as supplementary material when available.

Author contribution: Antonio Clareti Pereira conceived the study, performed the calculations, interpreted the data, prepared the figures and tables, and wrote the manuscript.

REFERENCES

1. Acquah, G., Abaka-Wood, G. B., Addai-Mensah, J., & Asamoah, R. (2025). Selective comminution for upgrading nickel and cobalt in nickel laterite ores. *Minerals Engineering, 233*, Article 109667. https://doi.org/10.1016/j.mineng.2025.109667

International Journal of Current Science Research and Review
ISSN: 2581-8341
Volume 09 Issue 07 July 2026
DOI: 10.47191/ijcsrr/V9-i7-27, Impact Factor: 8.048
IJCSRR @ 2026
www.ijcsrr.org

2. Acquah, G., Skinner, W., Abaka-Wood, G., Spiridonov, P., Addai-Mensah, J., & Asamoah, R. (2026). Extraction of nickel and cobalt from complex low-grade lateritic ores: Challenges and opportunities. *Minerals, 16*(3), Article 287. https://doi.org/10.3390/min16030287
3. Agatzini-Leonardou, S., Oustadakis, P., Dimaki, D., Zafiratos, J., Tsakiridis, P., Karidakis, T., Frogoudakis, E., & Drougas, J. (2021). Heap leaching of Greek low-grade nickel oxide ores by dilute sulphuric acid at a pilot-plant scale. *Materials Proceedings, 5*(1), Article 65. https://doi.org/10.3390/materproc2021005065
4. Basuhi, R., Bhuwalka, K., Moore, E., Diersen, I., [oito autores não recuperados]. (2024). Clean energy demand must secure sustainable nickel supply. *Joule, 8*(11). https://doi.org/10.1016/j.joule.2024.10.008.
5. Binnemans, K., Jones, P.T. The Twelve Principles of Circular Hydrometallurgy. *J. Sustain. Metall.* **9**, 1–25 (2023). https://doi.org/10.1007/s40831-022-00636-3.
6. Boafo, K., Borkar, P., & Eisele, T. (2026). Overcoming the iron selectivity hurdle in nickel bioleaching: A critical review of mechanisms, economic challenges, and future research directions. *Mineral Processing and Extractive Metallurgy Review*. Advance online publication. https://doi.org/10.1080/08827508.2026.2638765
7. Bonfu, B. A. A., Merah, M., Nakhaei, F., Alagha, L., Moats, M., & Awuah-Offei, K. (2026). Current state of hydrometallurgical processing for the recovery of nickel and cobalt from primary and secondary sources: Part I—Resources and market context, physical beneficiation, and leaching strategies. *Mineral Processing and Extractive Metallurgy Review*. Advance online publication. https://doi.org/10.1080/08827508.2026.2669914
8. Botelho Junior, A. B., Tenório, J. A. S., & Espinosa, D. C. R. (2023). Separation of critical metals by membrane technology under a circular economy framework: A review of the state-of-the-art. *Processes, 11*(4), Article 1256. https://doi.org/10.3390/pr11041256
9. Caetano, G. C., Ostroski, I. C., & Barros, M. A. S. D. (2025). Lateritic nickel and cobalt recovery routes: Strategic technologies. *Mineral Processing and Extractive Metallurgy Review, 46*(3), 400–414. https://doi.org/10.1080/08827508.2024.2328696
10. Chi, D., Yu, J., [três autores não informados], & Li, Y. (2026). Hydrometallurgical technologies of limonitic nickel laterite ore for carbon-neutral metallurgy: A review. *JOM*. Advance online publication. https://doi.org/10.1007/s11837-026-08139-2.
11. Connelly, D. (2025). The challenges for pressure leaching of nickel. In *Ni-Co 2025: 6th International Symposium on Nickel and Cobalt* (pp. 341–357). Springer. https://doi.org/10.1007/978-3-032-00167-2_27
12. Özsoy, B., & Can, İ. B. (2022). Effects of staged-addition of acid on high Ni Co recovery and low scale formation in HPAL of a lateritic ore. *Hydrometallurgy, 213*, Article 105935. https://doi.org/10.1016/j.hydromet.2022.105935
13. .Foss, M. M., & Koelsch, J. (2022, September). *Need nickel? How electrifying transport and Chinese investment are playing out in the Indonesian archipelago* [Technical report]. Rice University. https://doi.org/10.25613/30S0-Y623
14. Jeong, H.-E., Kang, H., Choi, S., & Kim, H. (2025). Comparative study of limonitic and saprolitic laterite ores on the leaching characteristics under atmospheric pressure. *Minerals Engineering, 226*, Article 109250. https://doi.org/10.1016/j.mineng.2025.109250
15. Kalupahana, R., Dushyantha, N., & Ratnayake, A. S. (2025). Circular hydrometallurgy to overcome the limitations of conventional extractive metallurgy. *Journal of Sustainable Metallurgy, 11*(4), 3322–3342. https://doi.org/10.1007/s40831-025-01247-4
16. Kang, H., Kim, J., Lee, J., Lee, D., Jeong, H.-E., & Kim, H. (2026). Early-stage temperature-dependent leaching kinetics and mechanisms of saprolitic and limonitic nickel laterite ores under atmospheric conditions. *Minerals Engineering, 239*, Article 110115. https://doi.org/10.1016/j.mineng.2026.110115
17. .Lasut, D. B. E., Kurniawati, R., Dahani, W., & Subandrio. (2023). The effect of concentration and temperature on nickel extraction from laterite nickel ore using atmospheric pressure acid leaching method. *AIP Conference Proceedings, 2646*(1), Article 050104. https://doi.org/10.1063/5.0112880
18. Lei, M., Ma, B., Chen, Y., Liu, W., Liu, B., Lv, D., ... & Wang, C. (2020). Effective separation and beneficiation of iron and chromium from laterite sulfuric acid leach residue. *ACS Sustainable Chemistry & Engineering*, *8*(9), 3959-3968.

International Journal of Current Science Research and Review
ISSN: 2581-8341
Volume 09 Issue 07 July 2026
DOI: 10.47191/ijcsrr/V9-i7-27, Impact Factor: 8.048
IJCSRR @ 2026
www.ijcsrr.org

19. Msumange, D. A., Jampaiah, D., Tardio, J., Nilsson, M., Arandiyan, H., & Bhargava, S. K. (2026). A review of nickel and cobalt from laterite ores: Toward sustainable extraction pathways for the battery industry. *Journal of Sustainable Metallurgy, 12*(2), 1038–1069. https://doi.org/10.1007/s40831-026-01439-6
20. .O'Sullivan, O., & Williams, I. (2025). Innovations in nickel leaching leading to minimal waste. In Metallurgy and Materials Society of CIM (Ed.), *Proceedings of the 63rd Conference of Metallurgists, COM 2024* (pp. 1855–1863). Springer. https://doi.org/10.1007/978-3-031-67398-6_299
21. Pereira, A. C. (2026b). Balancing nickel recovery, iron dissolution, acid dosage, and residence time in atmospheric sulfuric acid leaching of a ferruginous lateritic nickel ore. Journal International Review of Research Studies, 1(9), 1–30. https://doi.org/10.66104/dempc459
22. Pereira, A. C. (2026b). Quantification of $BaCl_2$-remobilizable nickel in atmospheric sulfuric leaching residues from ferruginous nickel ores using barium chloride as a sulfate probe. *International Review of Research Studies, 1*(9). https://doi.org/10.66104/x7rh8151
23. Prameswara, G., Bow, Y., Gustiana, H.S.E.A. *et al.* Fe Removal Strategy from Morowali Laterite Pregnant Leach Solution: Optimization and Kinetic Study. *Trans Indian Inst Met* **78**, 226 (2025). https://doi.org/10.1007/s12666-025-03705-9.
24. Ribeiro, G. da S., de Deus Nascimento, N., da Silveira Ribeiro, R., de Paole Moreira Miranda, M., Martins, P. R., Caetano, G. C., Alves de Andrade, L., & Ostroski, I. C. (2025). Optimization of the atmospheric acid leaching process for the recovery of nickel and cobalt from iron-rich lateritic ore. *Mining, Metallurgy & Exploration, 42*, 1127–1140. https://doi.org/10.1007/s42461-025-01233-0
25. Santos, A. L. A., Becheleni, E. M. A., Viana, P. R. M., Papini, R. M., Silvas, F. P. C., & Rocha, S. D. F. (2021). Kinetics of atmospheric leaching from a Brazilian nickel laterite ore allied to redox potential control. *Mining, Metallurgy & Exploration, 38*, 187–201. https://doi.org/10.1007/s42461-020-00310-w
26. Stanković, S., Kamberović, Ž., Friedrich, B., Stopić, S. R., Sokić, M., Marković, B., & Schippers, A. (2022). Options for hydrometallurgical treatment of Ni-Co lateritic ores for sustainable supply of nickel and cobalt for European battery industry from South-Eastern Europe and Turkey. *Metals, 12*(5), Article 807. https://doi.org/10.3390/met12050807
27. Suleimen, B., Adilov, G., Abdirashit, A., Kosdauletov, N., Kelamanov, B., Yessengaliyev, D., Arystanbayeva, A., & Abilberikova, A. (2026). Comparative review of processing technologies for oxidized (lateritic) nickel ores. *Applied Sciences, 16*(9), Article 4478. https://doi.org/10.3390/app16094478
28. Wang, W.-W., Liu, C., Qin, B., Liu, Z.-B., Li, X.-Y., Li, M.-C., Liu, G., Lv, D., Lu, Y.-D., Liu, J., & Chen, S.-X. (2025). Comprehensive recovery of valuable metals from laterite via neutralization sludge. *Separation and Purification Technology, 368*, Article 133006. https://doi.org/10.1016/j.seppur.2025.133006
29. Wen, J., Tran, T. T., & Lee, M. S. (2025). Recovery of pure Co(II) and Ni(II) solutions from synthetic sulfate leach liquor of laterite ores by precipitation and solvent extraction. *Mineral Processing and Extractive Metallurgy Review, 46*(4), 492–501. https://doi.org/10.1080/08827508.2024.2346652.

Cite this Article: Pereira, A.C. (2026). Linking Empirical Nickel Laterite Leaching Responses to Preliminary Economic Performance: Trade-Offs among Ni-Co Extraction, Acid Dosage, Fe Dissolution, and Residence Time. International Journal of Current Science Research and Review, 9(7), pp. 3865-3879. DOI: https://doi.org/10.47191/ijcsrr/V9-i7-27